Test Cases for the Geometrically-Nonlinear CBEAM3 Element

August 27, 2011

1 Isotropic Cantilever beam (NCB1)

This case is defined as in Geradin and Cardona (2001, p. 133). It is a cantilever beam of length $L = 5$ m, stiffness constants: $EA = 4.8 \times 10^8$ N, $GA = 3.231 \times 10^8$ N (in both axes), $GJ = 1.0 \times 10^6$ Nm, $EI = 9.346 \times 10^6$ Nm (in both axes), and mass constants $m = 100$ kg/m and $J = 10$ kgm.

1.1 Static Results

Table 1 shows the geometrically-nonlinear tip displacements for different discretizations under a dead vertical tip force of 600 kN. The convergence parameter in the nonlinear static equilibrium is 10^{-5}.

Table 1: NCB1 static test case: Tip displacements and rotations under tip dead force (600 kN)

Model	u_1 (m)	u_3 (m)	Ψ_2 (rad)
5 elements, 2 nodes	0.586	2.147	-0.6745
10 elements, 2 nodes	0.594	2.156	-0.6726
20 elements, 2 nodes	0.596	2.159	-0.6722
2 elements, 3 nodes	0.550	2.070	-0.6576
5 elements, 3 nodes	0.589	2.144	-0.6700
10 elements, 3 nodes	0.596	2.159	-0.6719
(Geradin and Cardona, 2001)		2.159	-0.6720

Figure 1 includes the deformed shapes obtained with tip follower forces and moments of up to 10000 kN and -15000 kNm, respectively. The tip position and rotation for different tip forces and discretizations is shown in Table 2. All results are obtained with 10 load substeps and a convergence parameter of 10^{-4}. The tip rotation obtained by a given tip moment M_2 in Figure 1(b) can be obtained analytically as $\Psi_2 = \frac{LM_2}{EI}$.

Table 2: NCB1 static test case: Tip position and rotations under tip follower force.

Force	Model	R_1 (m)	R_3 (m)	Ψ_2 (rad)
3000 kN	50 elements, 2 nodes	-0.3891	3.1246	-2.7611
3000 kN	50 elements, 3 nodes	-0.3900	3.1228	-2.7614
5000 kN	50 elements, 2 nodes	-0.0648	2.2485	-3.1404
5000 kN	50 elements, 3 nodes	-0.0641	2.2457	-3.1404
5000 kN	200 elements, 2 nodes	-0.0642	2.2459	-3.1404
5000 kN	200 elements, 3 nodes	-0.0641	2.2457	-3.1404
10000 kN	50 elements, 2 nodes	2.3372	-0.0982	-2.1037
10000 kN	50 elements, 3 nodes	2.3336	-0.1051	-2.1018
10000 kN	100 elements, 3 nodes	2.3336	-0.1051	-2.1018

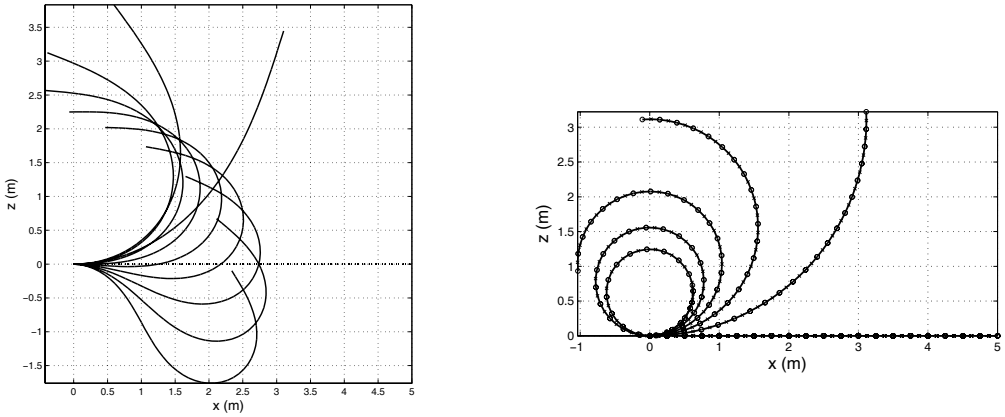

(a) Tip force up to 10000 kN, in increments of 1000 kN (50 2-noded elements)

(b) Tip moment up to -15000 kNm, in increments of -3000 kN (20 3-noded elements)

Figure 1: NCB1 static test case: Deformed shapes for increasing tip follower force and moment.

The interpolation of the Cartesian Rotation Vector is a critical issue, as it should guarantee *objectivity*, that is, invariance of the strain field under rigid-body rotations (Crisfield and Jelenic, 1999; Bauchau et al., 2008). This effect is investigated in the results of Table 3, which are obtained solving the cantilever beam under a tip following force of 3000 kN for different azimuth locations, ϕ, in the $x-y$ plane. The CRV in the solution includes the azimuth angle, and results in the table are rotated back to the plane of the undeformed beam. As it can be seen, the quadratic interpolation on the three-noded element provides a much better approximation of the CRV than the linear interpolation on the two-noded element.

Table 3: NCB1 static test case: Tip rotations (in the plane of the undeformed beam) under a tip follower force of 3000 kN and for varying azimuth orientations of the undeformed beam in the $x-y$ plane.

Azimuth	Model	Ψ_1 (rad)	Ψ_2 (rad)	Ψ_3 (rad)
0°	50 elements, 3 nodes	0	-2.7614	0
90°	50 elements, 3 nodes	5.577×10^{-8}	-2.7614	-4.085×10^{-7}
180°	50 elements, 3 nodes	1.408×10^{-8}	-2.7614	-6.938×10^{-7}
0°	100 elements, 2 nodes	0	-2.7613	0
90°	100 elements, 2 nodes	9.625×10^{-5}	-2.7613	-1.024×10^{-3}
180°	100 elements, 2 nodes	-3.812×10^{-5}	-2.7612	-1.336×10^{-3}
0°	10 elements, 3 nodes	0	-2.7553	0
90°	10 elements, 3 nodes	2.339×10^{-5}	-2.7553	-1.621×10^{-4}
180°	10 elements, 3 nodes	4.858×10^{-6}	-2.7553	-3.010×10^{-4}
0°	20 elements, 2 nodes	0	-2.7597	0
15°	20 elements, 2 nodes	5.306×10^{-4}	-2.7596	-4.583×10^{-3}
90°	20 elements, 2 nodes	2.333×10^{-3}	-2.7589	-2.453×10^{-2}
180°	20 elements, 2 nodes	-7.965×10^{-4}	-2.7562	-3.235×10^{-2}

1.2 Dynamic results

The natural frequencies for this beam are shown in Table 4. They are obtained with 100 2-noded elements, and for two situations: 1) undeformed beam and 2) deformed beam under a tip dead force of 600 kN (as in Table 1). The results for the undeformed beam are compared with the analytical expressions from the Euler-Bernoulli model. The results of the deformed beam were obtained using the actual tangent stiffness matrix (including both geometric and material terms).

Table 4: NCB1 dynamic test case: Natural angular frequencies (in rad/s) of the undeformed beam and with a tip follower force.

Model	Analytical	FEM	
Load	F=0	F=0	F=600 kN
1^{st} bending (xy)	43.0	42.5	46.5
1^{st} bending (xz)	43.0	42.5	49.1
1^{st} torsion	99.3	99.3	99.4
2^{nd} bending (xz)	269.4	249.6	243.9
2^{nd} bending (xy)	269.4	249.6	254.7
2^{nd} torsion	298.0	298.1	298.4
3^{rd} torsion	496.7	497.0	496.8
1^{st} axial	699.9	688.3	791.9

Finally, Figure 2 includes the time history of the non-zero beam tip displacements and rotations for a ramped harmonic tip vertical dead force of amplitude 60 kN and two different angular frequencies, Ω= 20 rad/s and Ω= 42.5 rad/s. Note that the second one lies near the first resonance frequency. The solution is obtained with 20 2-noded elements, time step 0.001s, and the force is ramped for $0 < t < 1$ s. Figure 2(a) includes results with the current displacement-based solution (*d-beam*) and an intrinsic beam model (*i-beam*) (Palacios and Cesnik, 2009) and Figure 2(b) compares linear and nonlinear results.

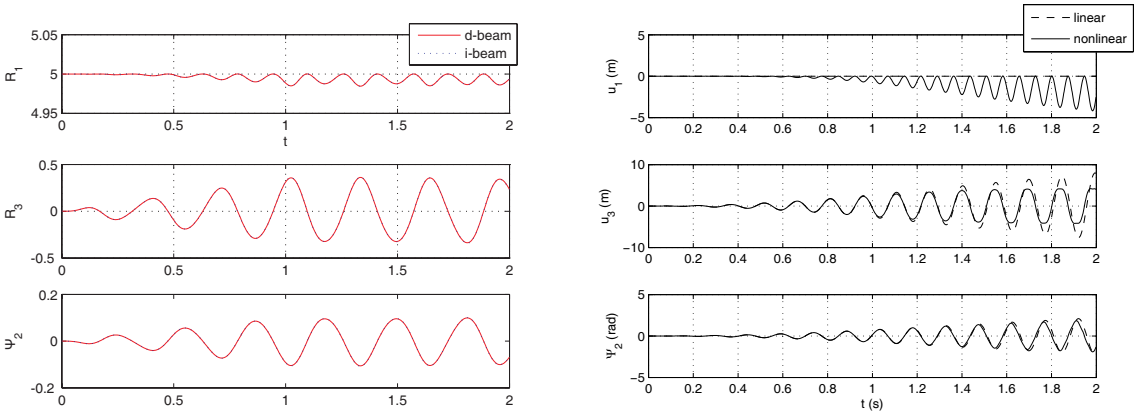

(a) Ω = 20 rad/s

(b) Ω = 42.5 rad/s

Figure 2: NCB1 dynamic test case: Tip positions/displacements and rotations for ramped harmonic dead tip load of 60 kN

2 L-Frame (LFRM)

A cantilever L-shape frame is now considered made of two beams like the one described above joined at a 90° angle and clamped at one end. Static results are obtained using 25 3-noded elements along each of the two beams and a convergence parameter of 10^{-4}. Figure 3 shows the static deformed shapes under a follower force at the free end. The convergence with the azimuth orientation of the undeformed beam is explored in Table 5.

3 45-degree bend (BEND)

This test case corresponds to a cantilever 45-degrees bend initially in the $x-y$ plane and subject to a tip follower force initially along the z axis (Geradin and Cardona, 2001, p. 133). The bend has a

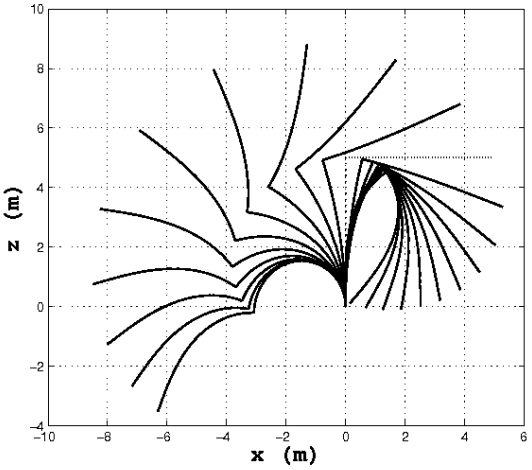

Figure 3: LFRM static test case: Deformed L-frame under static tip follower forces between -1 MN and 1 MN, in 0.1 MN intervals.

Table 5: LFRM static test case: Tip rotations (in the plane of the undeformed beam) under a tip follower force of 500 kN and for varying azimuth orientations of the undeformed beam in the $x-y$ plane.

Azimuth	Model	# iter	Ψ_1 (rad)	Ψ_2 (rad)	Ψ_3 (rad)
0°	2×25 elem, 3 nodes	10	0	-2.5041	0
90°	2×25 elem, 3 nodes	125	-2.034×10^{-7}	-2.5041	-8.926×10^{-8}
135°	2×25 elem, 3 nodes	200	-2.910×10^{-7}	-2.5041	-1.310×10^{-7}
180°	2×25 elem, 3 nodes	200	-3.278×10^{-7}	-2.5041	-1.547×10^{-7}
0°	2×10 elem, 3 nodes	10	0	-2.5015	0
90°	2×10 elem, 3 nodes	125	-1.055×10^{-5}	-2.5015	-4.352×10^{-6}
180°	2×10 elem, 3 nodes	200	-1.278×10^{-5}	-2.5015	-5.943×10^{-6}
0°	2×20 elem, 2 nodes	10	0	-2.5043	0
90°	2×20 elem, 2 nodes	125	-6.743×10^{-3}	-2.5037	-3.276×10^{-3}
180°	2×20 elem, 2 nodes	200	-1.489×10^{-2}	-2.5027	-6.937×10^{-3}

radius of 100 m, a square cross section of side 1 m, Youngs modulus E= 107 Pa and negligible Poisson ratio. Tables 6 shows the components of the displacements at the tip under dead forces for different discretizations, comparing with the results in the bibliography. Table 7 shows results for a tip follower force of 1000 N. It also shows both the numerical efficiency and the higher accuracy of using 3-noded elements to model curved beams. The convergence parameter was set up at 10^{-5} in all cases.

4 Vertical arch (ARCH)

This is a 180-degree arch with radius $R = 100$ m and clamped at both ends. It has a rectangular section of 2×1 m and isotropic material properties ($E = 10^7$ N, $G = 5 \times 10^6$ N). The arch is subject to a point vertical force, F, applied at its mid point. Figure 4 shows the displacements of the arch for increasing value of the force as they are obtained with 40 2- and 3-noded elements. *Snap-through* behavior occurs near the maximum load of 1750 N. Although special provisions are typically needed to catpure this behavior, the model with 3-noded element has captured it with only 5 load substeps. The 2-noded element was not able to capture this response. The position of the center point at the center point for different loading and discretizations is shown in Table 8.

Table 6: BEND static test case: Tip displacements under a 300-N tip dead force.

Model	u_1 (m)	u_2 (m)	u_3 (m)
NLCBEAM3 (2-noded 80 elem)	-7.45	-11.70	40.16
NLCBEAM3 (3-noded 80 elem)	-7.04	-11.93	40.19
Simo and Vu-Quoc (1986)	-6.96	-11.87	40.08
Geradin and Cardona (2001)	-7.15	-12.07	40.35

Table 7: BEND static test case: Tip displacement and rotation under a 1000-N tip follower force.

Nodes/Elem	Elements	u_1 (m)	u_2 (m)	u_3 (m)	Ψ_1 (rad)	Ψ_2 (rad)	Ψ_3 (rad)
2	10	-47.722	-69.127	50.296	1.7597	-2.0984	0.5626
2	20	-48.181	-69.533	49.663	1.7895	-2.0823	0.5608
2	40	-48.296	-69.635	49.501	1.8016	-2.0732	0.5591
2	100	-48.328	-69.663	49.456	1.8079	-2.0675	0.5578
2	200	-48.332	-69.667	49.449	1.8098	-2.0655	0.5573
3	5	-52.239	-67.583	48.331	1.6997	-2.1571	0.5624
3	10	-52.261	-67.591	48.298	1.7001	-2.1571	0.5626
3	20	-52.263	-67.591	48.296	1.7001	-2.1571	0.5626
3	100	-52.264	-67.591	48.296	1.7001	-2.1571	0.5626

5 Cantilever beam on a moving frame (NCB2)

This is a very flexible Titanium beam investigated by Pai (2007). Its dimensions are $479.0 \times 50.8 \times 0.45$ mm, with mass density 4430 kg/m3, Youngs modulus 127 GPa, and Poissons ratio 0.36. Experimental results were obtained on this beam clamped upwards on a moving base with harmonic motions. The weight loads on the beam are included as they may have a significant contribution in the amplitude of the out-of-plane motions.

Figure 5 includes the snapshots of the out-of-plane velocities along the beam during a cycle of base oscillations for two different frequencies and amplitudes. Numerical results are obtained with 40 2-noded elements, and with 100 time steps per cycle of excitation, and they are compared with the experimental results in Pai (2007, p. 392). To remove the transient dynamics, the base oscillations are slowly ramped up (for up to 250 cycles). The convergence parameter is set at 10^{-5} and the damping coefficient on the Newmark-β integration is 0.005.

References

O.A. Bauchau, A. Epple, and S. Heo. Interpolation of finite rotations in flexible multi-body dynamics simulations. *Proceedings of the Institution of Mechanical Engineers, Part K: Journal of Multi-body Dynamics*, 222(4):353–366, 2008. doi: 10.1243/14644193JMBD155.

M. A. Crisfield and Gordan Jelenic. Objectivity of strain measures in the geometrically exact three-dimensional beam theory and its finite-element implementation. *Proceedings of the Royal Society of London. Series A: Mathematical, Physical and Engineering Sciences*, 455(1983):1125–1147, 1999. doi: 10.1098/rspa.1999.0352.

M. Geradin and A. Cardona. *Flexible Multibody Dynamics : A Finite Element Approach.* John Wiley & Sons, Inc., New York, NY, USA, 2001.

P. F. Pai. *Highly Flexible Structures: Modeling, Computation, and Experimentation.* AIAA Education Series. American Institute of Aeronautics and Astronautics, Reston, Virginia, USA, 2007.

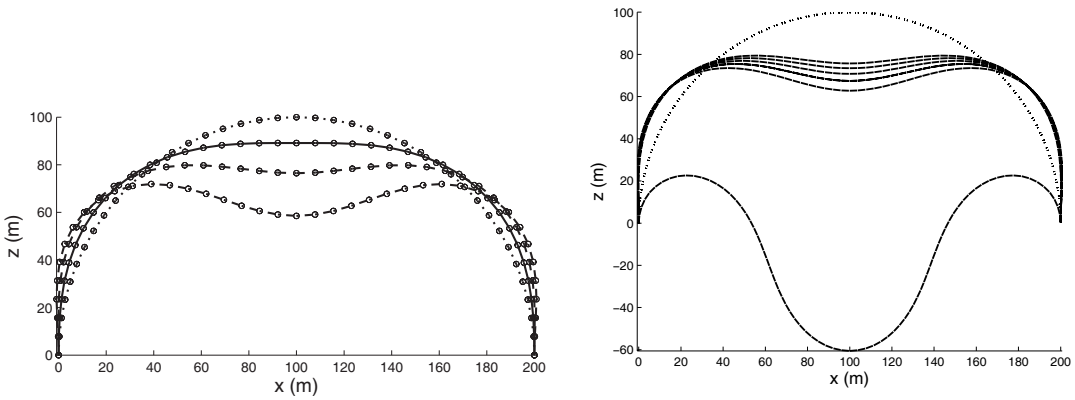

(a) 2-noded element;0, 1000 N, 1500 N, 1750 N

(b) 3-noded element; between 1500 N and 1750 N

Figure 4: ARCH static test case: Deformed shapes for increasing centre loads. 3-noded element captures snap-through behavior.

Table 8: Mid point vertical position

Nodes/Elem	Elements	F (N)	R_3 (m)
2	40	0	100.000
2	40	1000	89.151
2	40	1500	76.465
2	40	1750	58.512
3	40	1500	75.672
3	40	1550	73.420
3	40	1600	70.755
3	40	1650	67.434
3	40	1700	62.789
3	40	1750	-60.538

R. Palacios and C. E. S. Cesnik. Structural Models for Flight Dynamic Analysis of Very Flexible Aircraft. In *50th AIAA/ASME/ASCE/AHS/ASC Structures, Structural Dynamics and Materials Conference*, AIAA 2009-2403, Palm Springs, CA, USA, 4-7 May 2009.

J.C. Simo and L. Vu-Quoc. A three-dimensional finite-strain rod model. Part II: Computational aspects. *Computer Methods in Applied Mechanics and Engineering*, 58:79–116, 1986. doi: 10.1016/0045-7825(86)90079-4.

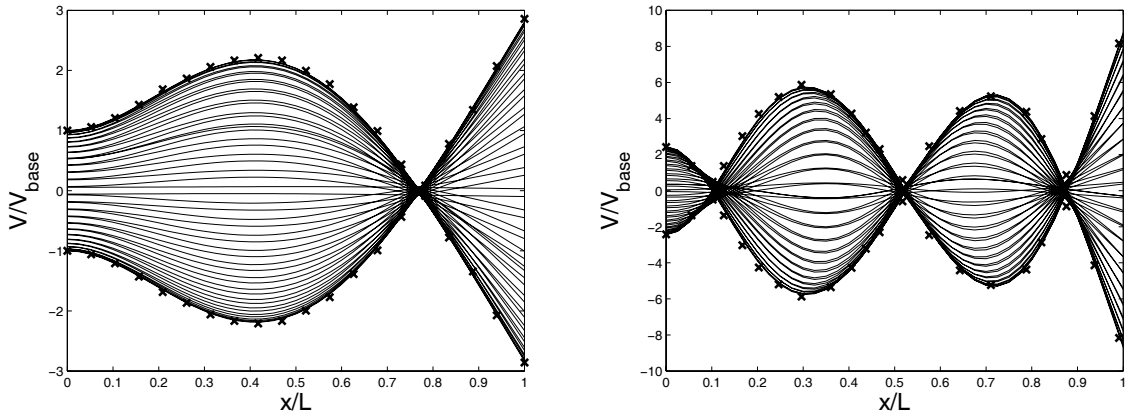

(a) $\Omega = 9$ Hz, $V_{base} = 0.1399$ m/s

(b) $\Omega = 32$ Hz, $V_{base} = 0.3414$ m/s

Figure 5: Out-of-plane velocity profiles at 50 consecutive steps during one period of base oscillations ($\times$: amplitudes in the experimental tests (Pai, 2007))